AIMS Mathematics, 11(4): 9470–9491.
DOI: 10.3934/math.2026392
Received: 18 January 2026
Revised: 12 March 2026
Accepted: 18 March 2026
Published: 09 April 2026

https://www.aimspress.com/journal/Math

Research article

Exploring the truncated M-fractional exact solitons, modulation instability, and stability analysis of the Kudryashov–Sinelshchikov model

Haitham Qawaqneh[1], Mostafa Abotaleb[2], Mohammed Ahmed Alomair[3,*] and Luai Abdulla Aldoghan[3]

[1] Department of Basic Science, Al-Zaytoonah University of Jordan, Amman 11733, Jordan
[2] Engineering School of Digital Technologies, Yugra State University, Khanty Mansiysk 628012, Russia
[3] Department of Quantitative Methods, School of Business, King Faisal University, Al-Ahsa 31982, Saudi Arabia

* **Correspondence:** Email: ma.alomair@kfu.edu.sa.

Abstract: In this paper, various types of exact soliton solutions of the truncated M-fractional Kudryashov–Sinelshchikov equation, a significant fluid surge model, were obtained. This model accounted for density and heat transfer effects while describing the propagation of pressure waves in mixtures of liquid–gas bubbles. By applying the modified (G'/G^2)-expansion method and the extended Sinh–Gordon equation expansion method, we derived new solutions in the forms of trigonometric, hyperbolic, and rational functions. The obtained solutions were illustrated dynamically using 2D, 3D, and contour plots. These results were novel due to the use of a new definition of fractional derivatives. The effect of the fractional derivative on the solutions was demonstrated through 2D plots. To examine the stability of the obtained solutions, stability analysis was performed. Steady-state solutions were derived using modulation instability analysis. The obtained solutions may be useful in various fields of science and engineering.

Keywords: Kudryashov–Sinelshchikov model; truncated M-fractional derivative; qualitative analysis; analytical techniques; exact solitons solutions
Mathematics Subject Classification: 35Q51, 35Q92, 35R11, 35R60, 60H15

1. Introduction

Fractional calculus deals with fractional derivatives and integrals, extending classical calculus to non-integer orders. It is useful for modeling complex systems with memory effects or nonlocal behavior and has applications in physics, engineering, finance, and many other fields. Various

nonlinear fractional models have been introduced in different areas, including the fractional Schrödinger equation was discussed in [1, 2]. The fractional coupled Boussinesq equation was explained in [3]. The fractional Riemann wave equation was used in [4]. The fractional generalized Bretherton equation was demonstrated in [5]. The fractional single-joint robot arm equation was discussed in [6]. The fractional Boussinesq–Burgers system was used in [7]. The fractional Schrödinger–Hirota equation was explained in [8]. The fractional Estevez–Mansfield–Clarkson equation was discussed in [9]. The fractional Rosenau–Burgers equation was used in [10]. The fractional low-pass electrical transmission line equation was demonstrated in [11].

Different analytical techniques have been developed to obtain exact soliton solutions, such as the unified technique was used in [12]. The Hirota bilinear method was utilized in [13, 14]. The extended simple equation technique was applied in [15]. The generalized first integral technique was used in [16]. The degenerate parabolic equation method was utilized in [17]. The modified simplest equation technique was applied in [18]. The variational method was used in [19]. The Hamiltonian-based method was discussed in [20]. The linear superposition and weight algorithm was used in [21]. The Fourier–Jacobi polynomial method was applied in [22].

In 2010, Kudryashov and Sinelshchikov first proposed the Kudryashov–Sinelshchikov model. This model is a nonlinear partial differential equation (PDE) that describes the evolution of nonlinear waves in a gas-liquid mixture. It takes into account factors such as interphase heat transfer, surface tension, and weak liquid compressibility. The model plays a significant role in understanding various physical phenomena, including nonlinear wave propagation in gas-liquid mixtures and related fluid dynamics processes. It also considers heat transfer and viscosity while describing the behavior of pressure waves in liquid-gas bubble mixtures [23].

A (1+1)-dimensional nonlinear Kudryashov–Sinelshchikov model is shown as [24]:

$$h_t + \theta_1 h h_x + h_{xxx} - \theta_2 (h h_{xx})_x - \theta_3 h_x h_{xx} - \theta_4 h_{xx} - \theta_5 (h h_x)_x = 0, \tag{1.1}$$

where $h(x,t)$ represents the profile describing the combined effects of density, heat transfer, and viscosity. The symbols $\theta_j, (j = 1, 2, \ldots, 5)$ denote real-valued constants that play a significant role in the structure of the considered equation. This model has been studied using various methods, such as the G'/G-expansion technique was used in [24]. The modified extended direct algebraic technique was used in [25]. The modified Khater technique was applied in [26]. The generalized exponential rational function technique was utilized in [27]. The Riccati–Bernoulli sub-ordinary differential equation (ODE) method was used in [28]. The simplest equation method was applied in [29]. The modern extension of the hyperbolic tanh function technique was applied in [30]. The finite element method with B-spline functions was used in [31]. The generalized unified method was utilized in [32]. The unified method was applied in [33]. The ansatz function method was used in [34].

We now discuss the following special cases according to the values of $\theta_j, (j = 1, 2, 3, 4, 5)$:

Case 1: If $\theta_j, (j = 2, 3, 4, 5)$ are all zero, then

$$h_t + \theta_1 h h_x + h_{xxx} = 0. \tag{1.2}$$

This equation is known as the Korteweg–de Vries equation.

Case 2: If $\theta_j, (j = 2, 3, 5)$ are all zero, then

$$h_t + \theta_1 h h_x + h_{xxx} - \theta_4 h_{xx} = 0. \tag{1.3}$$

Equation (1.3) is known as the Korteweg–de Vries–Burgers equation.

Case 3: If $\theta_1 = \theta_2 = 1$ and $\theta_4 = \theta_5 = 0$, then

$$h_t + hh_x + h_{xxx} - h_x h_{xxx} - \theta_3 h_x h_{xx} = 0. \tag{1.4}$$

Equation (1.4) is called the generalized Korteweg–de Vries–Burgers equation.

The nonlinear Kudryashov–Sinelshchikov equation in the framework of the truncated M-fractional derivative is given as follows:

$$\begin{aligned} &D^{\epsilon,\varrho}_{M,t}h + \theta_1 h D^{\epsilon,\varrho}_{M,x}h + D^{3\epsilon,\varrho}_{M,x}h - \theta_2 D^{\epsilon,\varrho}_{M,x}(hD^{2\epsilon,\varrho}_{M,x}h) \\ &- \theta_3(D^{\epsilon,\varrho}_{M,x}h)(D^{2\epsilon,\varrho}_{M,x}h) - \theta_4 D^{2\epsilon,\varrho}_{M,x}h - \theta_5 D^{\epsilon,\varrho}_{M,x}(hD^{\epsilon,\varrho}_{M,x}h) = 0. \end{aligned} \tag{1.5}$$

Equation (1.5) is obtained by replacing the partial derivatives in Eq (1.1) with partial fractional derivatives. The new version of the Kudryashov–Sinelshchikov model presented in Eq (1.5) has several advantages: (i) It provides a more accurate representation of the original model; (ii) it enables a better understanding of memory effects within the system; and (iii) it yields various exact soliton solutions along with numerical implementations, offering a more comprehensive understanding of the underlying phenomena.

The truncated M-fractional Kudryashov–Sinelshchikov model has many applications, such as:
(i) It is useful in ultrasound propagation and acoustic cavitation studies.
(ii) It describes viscous and compressible fluid flows where classical integer-order models fail.
(iii) It is applied to ion-acoustic and electrostatic wave propagation in plasmas with anomalous transport.
(iv) Fractional dynamics reflect the hereditary properties of biological media.
(v) It is suitable for fractured or porous geological formations where energy dissipation is non-classical.

Thus, the truncated M-fractional Kudryashov–Sinelshchikov model is particularly valuable in physical systems where nonlinear wave motion coexists with dissipation, dispersion, and memory effects, making it a versatile tool in acoustics, fluid dynamics, plasma physics, biological media, and geophysical wave analysis.

In this research, we employ the extended Sinh–Gordon equation expansion technique and the modified (G'/G^2)-expansion technique. Both methods have been widely used in the literature. For example, the extended Sinh–Gordon equation expansion technique has been applied to the Kundu–Eckhaus equation [35], nonlinear Schrödinger equation [36], the Φ^4 equation [37], and the new Hamiltonian amplitude equation [38], among others. Similarly, the modified (G'/G^2)-expansion technique has been used for the classical Boussinesq system [39], the Kadomtsev–Petviashvili modified equal width equation [40], the Wazwaz–Kaur–Boussinesq equation [41], and the coupled nonlinear Higgs equation [42], among others.

The main motivation of this research is to derive novel exact wave solutions of the nonlinear Kudryashov–Sinelshchikov equation in the framework of the truncated M-fractional derivative. The impact of the truncated M-fractional derivative on the obtained solutions is illustrated through 2D plots. The use of the truncated M-fractional derivative yields solutions that are closer to the numerical solutions of the governing model. Moreover, the truncated M-fractional derivative satisfies the

properties of both integer- and fractional-order derivatives. To the best of our knowledge, the obtained solutions have not been reported previously in the literature.

The stability of the obtained solutions is examined through stability analysis. In addition, modulation instability analysis is performed to derive the steady-state solutions of the considered system. Both techniques do not require any intermediate transformations and provide different types of exact soliton solutions, including dark, bright, periodic, kink, and singular solitons. Dark solitons have important applications in nonlinear optics, fluid dynamics, and plasma physics. Bright solitons are widely used in optical communications, nonlinear optics, and water wave studies. Kink solitons play significant roles in dislocation theory, ferromagnetism, superconductivity, and field theory. The employed methods are straightforward and effective for other nonlinear fractional models in applied sciences and engineering.

This paper is organized as follows: Section 2 presents the extended Sinh–Gordon equation expansion technique, the modified (G'/G^2)-expansion technique, and the derivation of exact wave solutions. Section 3 provides the graphical analysis. Section 4 presents the qualitative analysis. Section 5 discusses the results and findings. Finally, Section 6 concludes the paper.

Definition 1. Consider $w(y)$: $(0,\infty) \to \mathfrak{R}$, hence the truncated M-fractional derivative of w of degree ϵ [43]:

$$D_{M,y}^{\epsilon,\varrho} w(y) = \lim_{\delta \to 0} \frac{w\left(y\, E_\varrho(\delta y^{-\epsilon})\right) - w(y)}{\delta}, \quad \epsilon \in (0,1] and \;\; \varrho > 0,$$

where $E_\varrho(.)$ shows a truncated Mittag-Leffler function given in [44]:

$$E_\varrho(z) = \sum_{j=0}^{i} \frac{z^j}{\Gamma(\varrho j + 1)}, \;\; \varrho > 0, \;\; \text{and} \;\; z \in \mathbf{C},$$

Theorem 1. Suppose a,b $\in \mathfrak{R}$ and g, f are $\epsilon-$ differentiable for $y > 0$ from [43]:

$$(a)\; D_{M,y}^{\epsilon,\varrho}(ag(y) + bf(y)) = aD_{M,y}^{\epsilon,\varrho} g(y) + bD_{M,y}^{\epsilon,\varrho} f(y),$$
$$(b)\; D_{M,y}^{\epsilon,\varrho}(g(y).f(y)) = g(y)D_{M,y}^{\epsilon,\varrho} f(y) + f(y)D_{M,y}^{\epsilon,\varrho} g(y),$$
$$(c)\; D_{M,y}^{\epsilon,\varrho}\left(\frac{g(y)}{f(y)}\right) = \frac{f(y)D_{M,y}^{\epsilon,\varrho} g(y) - g(y)D_{M,y}^{\epsilon,\varrho} f(y)}{(f(y))^2},$$
$$(d)\; D_{M,y}^{\epsilon,\varrho}(C) = 0, \;\; \text{where } C \text{ is a constant},$$
$$(e)\; D_{M,y}^{\epsilon,\varrho} g(y) = \frac{y^{1-\epsilon}}{\Gamma(\varrho+1)} \frac{dg(y)}{dy}.$$

while ϵ shows the fractional order of the derivative. It controls the "degree" of differentiation between classical derivative 1 and integral-like behavior near 0.

ϱ is a positive parameter that generalizes the kernel via the Mittag-Leffler function. Typically, $\varrho > 0$. $\delta \to 0$ is a limiting process similar to the classical derivative definition.

2. Methodologies and exact wave solutions

2.1. Extended Sinh–Gordon equation expansion method

Here, there are some phases for this concerned method [45].

Phase 1. Suppose a fractional nonlinear PDE:

$$F(g, D^{\epsilon,\varrho}_{M,t}g^2, g^2 D^{\epsilon,\varrho}_{M,x}g, D^{\epsilon,\varrho}_{M,x}g, ...) = 0. \tag{2.1}$$

Here, g represents a function.

Use a following wave transformation [24] in the concept of a truncated M-fractional derivative:

$$g = G(\mho),\ \mho = \Gamma(1+\varrho)(\frac{x^\epsilon}{\epsilon} - \lambda\frac{t^\epsilon}{\epsilon}). \tag{2.2}$$

Using Eq (2.2) in Eq (2.1) provides

$$H(G, G^2G', G'', ...) = 0. \tag{2.3}$$

Phase 2. Assuming the solution of Eq (2.3) is mentioned,

$$G(f(\mho)) = a_0 + \sum_{j=1}^{m}(b_j \sinh(f(\mho)) + a_j \cosh(f(\mho)))^j. \tag{2.4}$$

Here, a_0, a_j, b_j $(j = 1, 2, 3, ..., m)$ are undetermined. The new function f of $\mho$ fulfills the given equation

$$\frac{df}{d\mho} = \sinh(f). \tag{2.5}$$

Equation (2.5) is gained by using the equation

$$q_{xt} = \kappa \sinh(v). \tag{2.6}$$

From [46], we gain the results for Eq (2.6) mentioned as

$$\sinh f(\mho) = \pm csch(\mho) \quad \text{or} \quad \cosh f(\mho) = \pm \coth(\mho) \tag{2.7}$$

and

$$\sinh f(\mho) = \pm i\ \text{sech}(\mho) \quad \text{or} \quad \cosh f(\mho) = \pm \tanh(\mho). \tag{2.8}$$

where $i^2 = -1$ in Eq (2.8).

Phase 3. Inserting Eqs (2.4) and (2.5) in Eq (2.3), we obtain the system of equations.

Phase 4. By solving the obtained system of equations, it provides values of unknowns. By applying achieved solutions, Eqs (2.7) and (2.8) give the solutions of Eq (2.3) mentioned as

$$G(\mho) = a_0 + \sum_{j=1}^{m}(\pm b_j csch(\mho) \pm a_j \coth(\mho))^j \tag{2.9}$$

and

$$G(\mho) = a_0 + \sum_{j=1}^{m}(\pm ib_j \text{sech}(\mho) \pm a_j \tanh(\mho))^j. \tag{2.10}$$

This method has some limitations. For example, (i) this method is more suitable for integrable equations. Non-integrable equations may not be easily solvable using this method. (ii) This method can generate exact solutions, but the physical interpretation of these solutions might be limited or require additional analysis. (iii) This method may involve solving algebraic equations with many terms, which can be computationally intensive and prone to errors.

2.2. The modified (G'/G^2)-expansion method

Now, some main steps of the method will be given [47].

Step 1. Consider Eqs (2.1)–(2.3).

Step 2. Consider the solution of Eq (2.3) shown as

$$Q(\eta) = \sum_{i=0}^{m} \alpha_i (\frac{G'}{G^2})^i, \tag{2.11}$$

where $\alpha_i (i = 0, 1, 2, 3, ..., m)$ are undetermined while α_i is nonzero. Another profile, $G = G(\eta)$, satisfies

$$(\frac{G'}{G^2})' = a + b(\frac{G'}{G^2})^2. \tag{2.12}$$

Here, a and b represent the parameters. Authors gain the below results for Eq (2.12) depending on a.

Case 1: $ab < 0$ yields

$$(\frac{G'}{G^2}) = -\frac{\sqrt{|ab|}}{b} + \frac{\sqrt{|ab|}}{2} \ (\frac{C_1 \sinh(\sqrt{ab}\ \eta) + C_2 \cosh(\sqrt{ab}\ \eta)}{C_1 \cosh(\sqrt{ab}\ \eta) + C_2 \sinh(\sqrt{ab}\ \eta)}). \tag{2.13}$$

Case 2: When $ab > 0$, we have

$$(\frac{G'}{G^2}) = \sqrt{\frac{a}{b}} \ (\frac{C_1 \cos(\sqrt{ab}\ \eta) + C_2 \sin(\sqrt{ab}\ \eta)}{C_1 \sin(\sqrt{ab}\ \eta) - C_2 \sin(\sqrt{ab}\ \eta)}). \tag{2.14}$$

Case 3: When a is zero and b is non-zero, we have

$$(\frac{G'}{G^2}) = -\frac{C_1}{b(C_1\eta + C_2)}. \tag{2.15}$$

Here, C_1 and C_2 are parameters.

Step 3. Insert Eq (2.11) into Eq (2.3) with Eq (2.12) and sum up the coefficients for every $(\frac{G'}{G^2})^i$. Putting each equal to zero then solves the achieved system.

Step 4. Putting Eq (2.11), of which α_i, ν are achieved in **Step 3**, into Eq (2.3), we obtain the solutions of Eq (2.1).

This method has many drawbacks or limitations, including: (i) This method involves tedious and complex calculations, particularly when dealing with higher-order derivatives or more intricate forms of $G(\eta)$. (ii) Some equations may not be amenable to a solution using this approach, especially if they have complex nonlinear terms or higher dimensions. (iii) The method may involve solving algebraic equations with many terms, which can be computationally intensive and prone to errors.

Assume the given relation

$$h = H(\mho), \qquad \mho = \Gamma(\varrho + 1)(\frac{x^\epsilon}{\epsilon} - \lambda\frac{t^\epsilon}{\epsilon}). \tag{2.16}$$

Here, H represents a wave shape, and λ indicates the fractional wave parameter controlling the propagation scale.

Using Eq (1.5), we get

$$D_{M,t}^{\epsilon,\varrho}h = -\lambda H', \quad D_{M,x}^{\epsilon,\varrho}h = H', \quad D_{M,x}^{2\epsilon,\varrho}h = H'',$$
$$D_{M,x}^{3\epsilon,\varrho}h = H''', \quad D_{M,x}^{\epsilon,\varrho}(hD_{M,x}^{2\epsilon,\varrho}h) = HH''' + H''H',$$
$$D_{M,x}^{\epsilon,\varrho}(hD_{M,x}^{\epsilon,\varrho}h) = HH'' + H''H', \quad (D_{M,x}^{\epsilon,\varrho}h)(D_{M,x}^{2\epsilon,\varrho}h) = H'H''.$$

Using the above obtained values in Eq (1.5), taking integration once, and assuming the integration constant is equal to 0 results in

$$H'' - \theta_2 HH'' + \frac{\theta_1 H^2}{2} - \theta_5 HH' - \frac{1}{2}\theta_3 (H')^2 - \theta_4 H' - H\lambda = 0. \tag{2.17}$$

We obtain $m = 1$ by balancing the highest derivative term H'' and the highest nonlinear term HH' with the use of the homogenous balance scheme in Eq (2.17).

2.3. Through extended Sinh–Gordon equation expansion scheme

Equation (2.4) changes into the given form if $m = 1$:

$$G(\mho) = a_0 + a_1 \cosh(f(\mho)) + b_1 \sinh(f(\mho)). \tag{2.18}$$

Using Eq (2.18) in Eq (2.17) along with Eq (2.5), we gain a system containing a_0, a_1, b_1, and λ. By simplifying the set, it provides the following sets:

Set 1.

$$a_0 = -\frac{4}{\theta_3 - 4\theta_5}, \quad a_1 = -\frac{4}{\theta_3 - 4\theta_5}, \quad b_1 = -\frac{4}{\theta_3 - 4\theta_5},$$
$$\lambda = \theta_4 + 1, \quad \theta_1 = -\frac{1}{4}(\theta_4 + 1)(\theta_3 - 4\theta_5), \quad \theta_2 = -\frac{\theta_3}{4}, \tag{2.19}$$

and

$$h_1(x,t) = -\frac{4}{\theta_3 - 4\theta_5}(1 \pm \coth(\Gamma(\varrho+1)(\frac{x^\epsilon}{\epsilon} - (\theta_4+1)\frac{t^\epsilon}{\epsilon})) \pm \operatorname{csch}(\Gamma(\varrho+1)(\frac{x^\epsilon}{\epsilon} - (\theta_4+1)\frac{t^\epsilon}{\epsilon}))), \tag{2.20}$$

$$h_2(x,t) = -\frac{4}{\theta_3 - 4\theta_5}(1 \pm \tanh(\frac{\Gamma(1+\varrho)}{\epsilon}(x^\epsilon - (\theta_4+1)t^\epsilon)) \pm i\operatorname{sech}(\Gamma(\varrho+1)(\frac{x^\epsilon}{\epsilon} - (\theta_4+1)\frac{t^\epsilon}{\epsilon}))). \tag{2.21}$$

Set 2.

$$a_0 = -\frac{4}{\theta_3 - 4\theta_5}, \quad a_1 = -\frac{4}{\theta_3 - 4\theta_5}, \quad b_1 = \frac{4}{\theta_3 - 4\theta_5},$$
$$\lambda = \theta_4 + 1, \quad \theta_1 = -\frac{1}{4}(\theta_4 + 1)(\theta_3 - 4\theta_5), \quad \theta_2 = -\frac{\theta_3}{4}, \tag{2.22}$$

and

$$h_1(x,t) = -\frac{4}{\theta_3 - 4\theta_5}(1 \pm \coth(\Gamma(\varrho+1))(\frac{x^\epsilon}{\epsilon} - (\theta_4+1)\frac{t^\epsilon}{\epsilon})) \mp \operatorname{csch}(\Gamma(\varrho+1)(\frac{x^\epsilon}{\epsilon} - (\theta_4+1)\frac{t^\epsilon}{\epsilon})), \tag{2.23}$$

$$h_2(x,t) = -\frac{4}{\theta_3 - 4\theta_5}(1 \pm \tanh(\Gamma(1+\varrho)(\frac{x^\epsilon}{\epsilon} - (\theta_4+1)\frac{t^\epsilon}{\epsilon})) \mp i\text{sech}(\Gamma(1+\varrho)(\frac{x^\epsilon}{\epsilon} - (\theta_4+1)\frac{t^\epsilon}{\epsilon}))). \quad (2.24)$$

Set 3.

$$a_0 = -\frac{4}{\theta_3 - 2\theta_5}, \quad a_1 = -\frac{4}{\theta_3 - 2\theta_5}, \quad b_1 = 0, \quad (2.25)$$

$$\lambda = 2(\theta_4+2), \quad \theta_1 = -\frac{1}{2}(\theta_4+2)(\theta_3 - 2\theta_5), \quad \theta_2 = -\frac{\theta_3}{4}, \quad (2.26)$$

and

$$h_1(x,t) = -\frac{4}{\theta_3 - 2\theta_5}(1 \pm \coth(\Gamma(1+\varrho)(\frac{x^\epsilon}{\epsilon} - 2(\theta_4+2)\frac{t^\epsilon}{\epsilon}))), \quad (2.27)$$

$$h_2(x,t) = -\frac{4}{\theta_3 - 2\theta_5}(1 \pm \tanh(\Gamma(1+\varrho)(\frac{x^\epsilon}{\epsilon} - 2(\theta_4+2)\frac{t^\epsilon}{\epsilon}))). \quad (2.28)$$

Set 4.

$$a_0 = -\frac{4}{\theta_3 + 2\theta_5}, \quad a_1 = \frac{4}{\theta_3 + 2\theta_5}, \quad b_1 = 0, \quad \lambda = 4 - 2\theta_4, \quad \theta_1 = \frac{1}{2}(\theta_4 - 2)(\theta_3 + 2\theta_5), \quad \theta_2 = -\frac{\theta_3}{4}, \quad (2.29)$$

and

$$h_1(x,t) = -\frac{4}{\theta_3 + 2\theta_5}(1 \mp \coth(\Gamma(1+\varrho)(\frac{x^\epsilon}{\epsilon} - (4-2\theta_4)\frac{t^\epsilon}{\epsilon}))), \quad (2.30)$$

$$h_2(x,t) = -\frac{4}{\theta_3 + 2\theta_5}(1 \mp \tanh(\Gamma(1+\varrho)(\frac{x^\epsilon}{\epsilon} - (4-2\theta_4)\frac{t^\epsilon}{\epsilon}))). \quad (2.31)$$

Set 5.

$$a_0 = -\frac{4}{\theta_3 + 4\theta_5}, \quad a_1 = \frac{4}{\theta_3 + 4\theta_5}, \quad b_1 = -\frac{4}{\theta_3 + 4\theta_5},$$
$$\lambda = 1 - \theta_4, \quad \theta_1 = \frac{1}{4}(\theta_4 - 1)(\theta_3 + 4\theta_5), \quad \theta_2 = -\frac{\theta_3}{4}, \quad (2.32)$$

and

$$h_1(x,t) = -\frac{4}{\theta_3 + 4\theta_5}(1 \mp \coth(\Gamma(1+\varrho)(\frac{x^\epsilon}{\epsilon} - (1-\theta_4)\frac{t^\epsilon}{\epsilon})) \pm \text{csch}(\Gamma(1+\varrho)(\frac{x^\epsilon}{\epsilon} - (1-\theta_4)\frac{t^\epsilon}{\epsilon}))), \quad (2.33)$$

$$h_2(x,t) = -\frac{4}{\theta_3 + 4\theta_5}(1 \mp \tanh(\Gamma(1+\varrho)(\frac{x^\epsilon}{\epsilon} - (1-\theta_4)\frac{t^\epsilon}{\epsilon})) \pm i\,\text{sech}(\Gamma(1+\varrho)(\frac{x^\epsilon}{\epsilon} - (1-\theta_4)\frac{t^\epsilon}{\epsilon}))). \quad (2.34)$$

Set 6.

$$a_0 = -\frac{4}{\theta_3 + 4\theta_5}, \quad a_1 = \frac{4}{\theta_3 + 4\theta_5}, \quad b_1 = \frac{4}{\theta_3 + 4\theta_5}, \quad (2.35)$$

$$\lambda = 1 - \theta_4, \quad \theta_1 = \frac{1}{4}(\theta_4 - 1)(\theta_3 + 4\theta_5), \quad \theta_2 = -\frac{\theta_3}{4}, \quad (2.36)$$

and

$$h_1(x,t) = \frac{4}{\theta_3 + 4\theta_5}(-1 \pm \coth(\Gamma(1+\varrho)(\frac{x^\epsilon}{\epsilon} - (1-\theta_4)\frac{t^\epsilon}{\epsilon})) \pm \text{csch}(\Gamma(1+\varrho)(\frac{x^\epsilon}{\epsilon} - (1-\theta_4)\frac{t^\epsilon}{\epsilon}))), \quad (2.37)$$

$$h_2(x,t) = \frac{4}{\theta_3 + 4\theta_5}(-1 \pm \tanh(\Gamma(1+\varrho)(\frac{x^\epsilon}{\epsilon} - (1-\theta_4)\frac{t^\epsilon}{\epsilon})) \pm i\text{sech}(\Gamma(1+\varrho)(\frac{x^\epsilon}{\epsilon} - (1-\theta_4)\frac{t^\epsilon}{\epsilon}))). \quad (2.38)$$

2.4. Through modified (G'/G^2)-expansion scheme

Equation (2.11) transforms to the given form if $m = 1$:

$$Q(\eta) = \alpha_0 + \alpha_1 \frac{G'(\eta)}{G^2(\eta)}. \tag{2.39}$$

Here, α_0 and α_1 are unknowns. Using Eq (2.39) along Eq (2.12) and with the help of Maple software, it provides the following different sets:

Set 1.

$$\alpha_0 = -\frac{4\sqrt{ab}}{\sqrt{ab}\theta_3 - 2i\theta_5}, \quad \alpha_1 = -\frac{4ib}{\sqrt{ab}\theta_3 - 2i\theta_5}, \quad \lambda = -4ab - 2i\sqrt{ab}\theta_4,$$
$$\theta_1 = \frac{1}{2}\left(2\sqrt{ab} + i\theta_4\right)\left(\sqrt{ab}\theta_3 - 2i\theta_5\right), \quad \theta_2 = -\frac{\theta_3}{4}. \tag{2.40}$$

Case 1:

$$\begin{aligned} h(x,t) = -\frac{4}{\sqrt{ab}\theta_3 - 2i\theta_5}(\sqrt{ab} + ib(-\frac{\sqrt{|ab|}}{b} + \frac{\sqrt{|ab|}}{2}((C_1\sinh(\sqrt{ab}\frac{\Gamma(1+\varrho)}{\epsilon} \\ (x^\epsilon - (-4ab - 2i\sqrt{ab}\theta_4)t^\epsilon)) + C_2\cosh(\sqrt{ab}\frac{\Gamma(1+\varrho)}{\epsilon} \\ (x^\epsilon - (-4ab - 2i\sqrt{ab}\theta_4)t^\epsilon)))/(C_1\cosh(\sqrt{ab}\frac{\Gamma(\varrho+1)}{\epsilon}(x^\epsilon - (-4ab - 2i\sqrt{ab}\theta_4)t^\epsilon)) \\ + C_2\sinh(\sqrt{ab}\frac{\Gamma(\varrho+1)}{\epsilon}(x^\epsilon - (-4ab - 2i\sqrt{ab}\theta_4)t^\epsilon)))))). \end{aligned} \tag{2.41}$$

Case 2:

$$\begin{aligned} h(x,t) = -\frac{4}{\sqrt{ab}\theta_3 - 2\iota\theta_5}(\sqrt{ab} + ib(\sqrt{\frac{a}{b}}((C_1\cos(\sqrt{ab}\frac{\Gamma(1+\varrho)}{\epsilon}(x^\epsilon - (-4ab - 2i\sqrt{ab}\theta_4)t^\epsilon)) \\ + C_2\sin(\sqrt{ab}\frac{\Gamma(1+\varrho)}{\epsilon}(x^\epsilon - (-4ab - 2i\sqrt{ab}\theta_4)t^\epsilon)))/(C_1\sin(\sqrt{ab}\frac{\Gamma(\varrho+1)}{\epsilon} \\ (x^\epsilon + (4ab + 2i\sqrt{ab}\theta_4)t^\epsilon)) - C_2\sin(\sqrt{ab}\frac{\Gamma(\varrho+1)}{\epsilon}(x^\epsilon - (-4ab - 2i\sqrt{ab}\theta_4)t^\epsilon)))))). \end{aligned} \tag{2.42}$$

Set 2.

$$\alpha_0 = -\frac{4\sqrt{ab}}{\sqrt{ab}\theta_3 + 2i\theta_5}, \quad \alpha_1 = \frac{4ib}{\sqrt{ab}\theta_3 + 2i\theta_5}, \quad \lambda = -4ab + 2i\sqrt{ab}\theta_4,$$
$$\theta_1 = \frac{1}{2}(2\sqrt{ab} - i\theta_4)(\sqrt{ab}\theta_3 + 2i\theta_5), \quad \theta_2 = -\frac{\theta_3}{4}. \tag{2.43}$$

Case 1:

$$\begin{aligned} h(x,t) = -\frac{4}{\sqrt{ab}\theta_3 + 2i\theta_5}(\sqrt{ab} - ib(-\frac{\sqrt{|ab|}}{b} + \frac{\sqrt{|ab|}}{2}((C_1\sinh(\sqrt{ab}\frac{\Gamma(1+\varrho)}{\epsilon}(x^\epsilon \\ - (-4ab + 2i\sqrt{ab}\theta_4)t^\epsilon)) + C_2\cosh(\sqrt{ab}\frac{\Gamma(1+\varrho)}{\epsilon}(x^\epsilon - (-4ab \end{aligned}$$

$$+ 2i\sqrt{ab}\theta_4)t^\epsilon)))/(C_1\cosh(\sqrt{ab}\frac{\Gamma(1+\varrho)}{\epsilon}(x^\epsilon - (-4ab + 2i\sqrt{ab}\theta_4)t^\epsilon))$$
$$+ C_2\sinh(\sqrt{ab}\frac{\Gamma(1+\varrho)}{\epsilon}(x^\epsilon - (-4ab + 2i\sqrt{ab}\theta_4)t^\epsilon))))))). \quad (2.44)$$

Case 2:

$$h(x,t) = -\frac{4}{\sqrt{ab}\theta_3 + 2i\theta_5}(\sqrt{ab} - ib(\sqrt{\frac{a}{b}}((C_1\cos(\sqrt{ab}\frac{\Gamma(1+\varrho)}{\epsilon}(x^\epsilon - (-4ab + 2i\sqrt{ab}\theta_4)t^\epsilon))$$
$$+ C_2\sin(\sqrt{ab}\frac{\Gamma(1+\varrho)}{\epsilon}(x^\epsilon - (-4ab + 2i\sqrt{ab}\theta_4)t^\epsilon)))/(C_1\sin(\sqrt{ab}\frac{\Gamma(1+\varrho)}{\epsilon}(x^\epsilon - (-4ab$$
$$+ 2i\sqrt{ab}\theta_4)t^\epsilon)) - C_2\sin(\sqrt{ab}\frac{\Gamma(\varrho+1)}{\epsilon}(x^\epsilon - (-4ab + 2i\sqrt{ab}\theta_4)t^\epsilon))))))). \quad (2.45)$$

3. Graphical description

Here, we present several graphs to demonstrate the physical behavior of the solutions (see Figure 1).

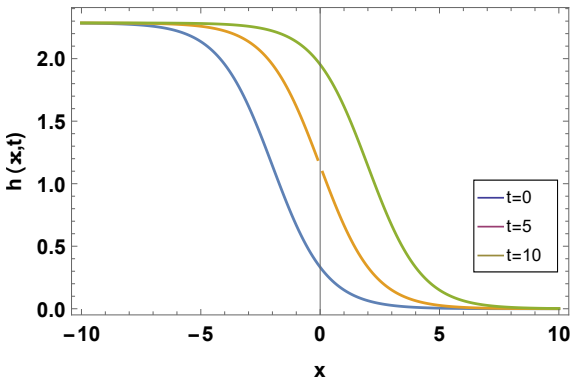

(a) 2D graph.

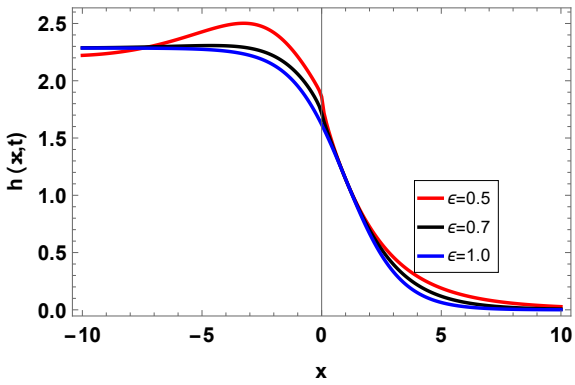

(b) 2D graph.

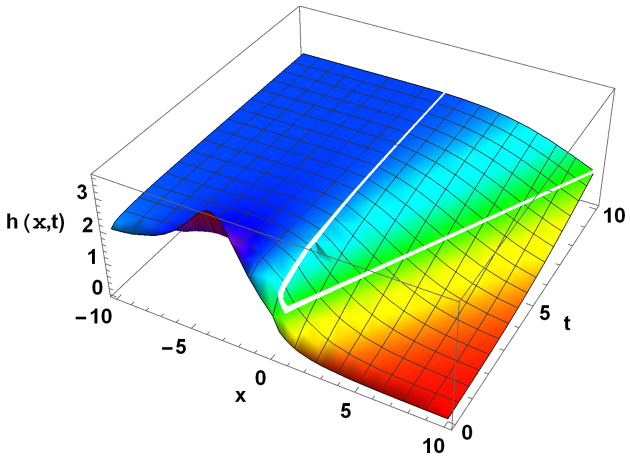

(c) 3D plot at $\epsilon = 0.6$

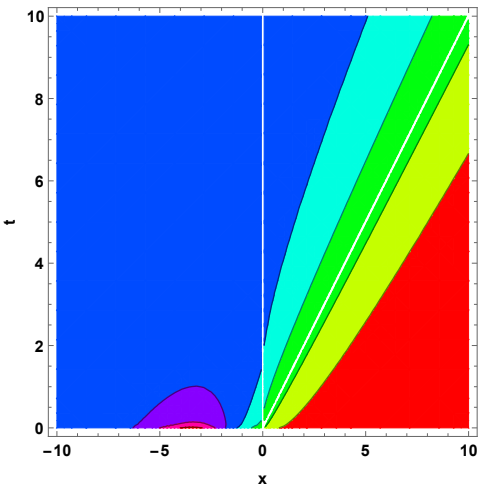

(d) Contour plot when $\epsilon = 0.6$

Figure 1. Physical behavior of $h(x, t)$ denoted through Eq (2.20) when $\theta_3 = 0.5$, $\theta_4 = -0.001$, $\theta_5 = 1$, and $\varrho = 0.5$.

The above graphs show the singular wave solution. Figure 1a shows the 2D graph for the variation of time when $x \in (-10, 10)$. We can observe that the phase of the wave changes with the change in the values of t. Figure 1b represents the 2D graph for the variation of ϵ when $x \in (-10, 10)$. It is seen that the phase of the wave changes with the change in the value of ϵ. Figure 1c shows the 3D graph for $\epsilon = 0.6$ when $x \in (-10, 10)$ and $t \in (0, 10)$. Figure 1d denotes the contour graph for $\epsilon = 0.6$ when $x \in (-10, 10)$ and $t \in (0, 10)$.

The following graphs show the bright-dark soliton solution. Figure 2a shows the 2D graph for the variation of time when $x \in (-12, 12)$. We can observe that the phase of the wave changes with the change in the values of t. Figure 2b represents the 2D graph for the variation of ϵ when $x \in (-12, 12)$. It is seen that the phase of the wave changes with the change in the value of ϵ. Figure 2c shows the 3D graph for $\epsilon = 0.6$ when $x \in (-12, 12)$ and $t \in (0, 10)$. Figure 2d denotes the contour graph for $\epsilon = 0.6$ when $x \in (-12, 12)$ and $t \in (0, 10)$.

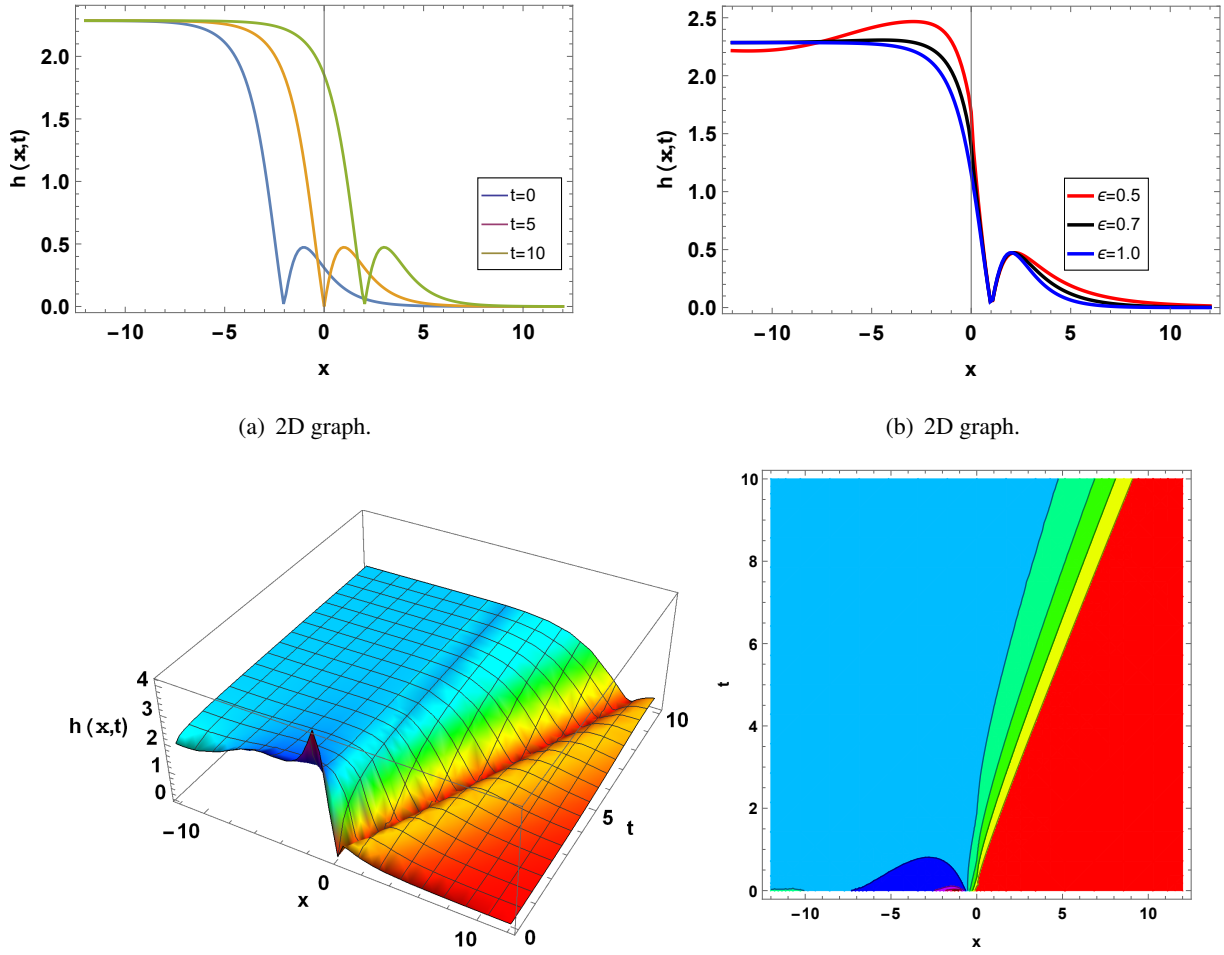

(a) 2D graph.

(b) 2D graph.

(c) 3D plot at $\epsilon = 0.6$

(d) Contour plot when $\epsilon = 0.6$

Figure 2. Physical behavior of $h(x, t)$ denoted through Eq (2.21) for $\theta_3 = 0.5$, $\theta_4 = 0.01$, $\theta_5 = 1$, and $\varrho = 0.5$.

The following graphs represent the dark soliton solution. Figure 3a shows the 2D graph for the

variation of time when $x \in (-5, 5)$. We can observe that the phase of the wave changes with the change in the values of t. Figure 3b represents the 2D graph for the variation of ϵ when $x \in (-5, 5)$. It is seen that the phase of the wave changes with the change in the value of ϵ. Figure 3c shows the 3D graph for $\epsilon = 0.6$ when $x \in (-5, 5)$ and $t \in (0, 10)$. Figure 3d denotes the contour graph for $\epsilon = 0.6$ when $x \in (-5, 5)$ and $t \in (0, 10)$.

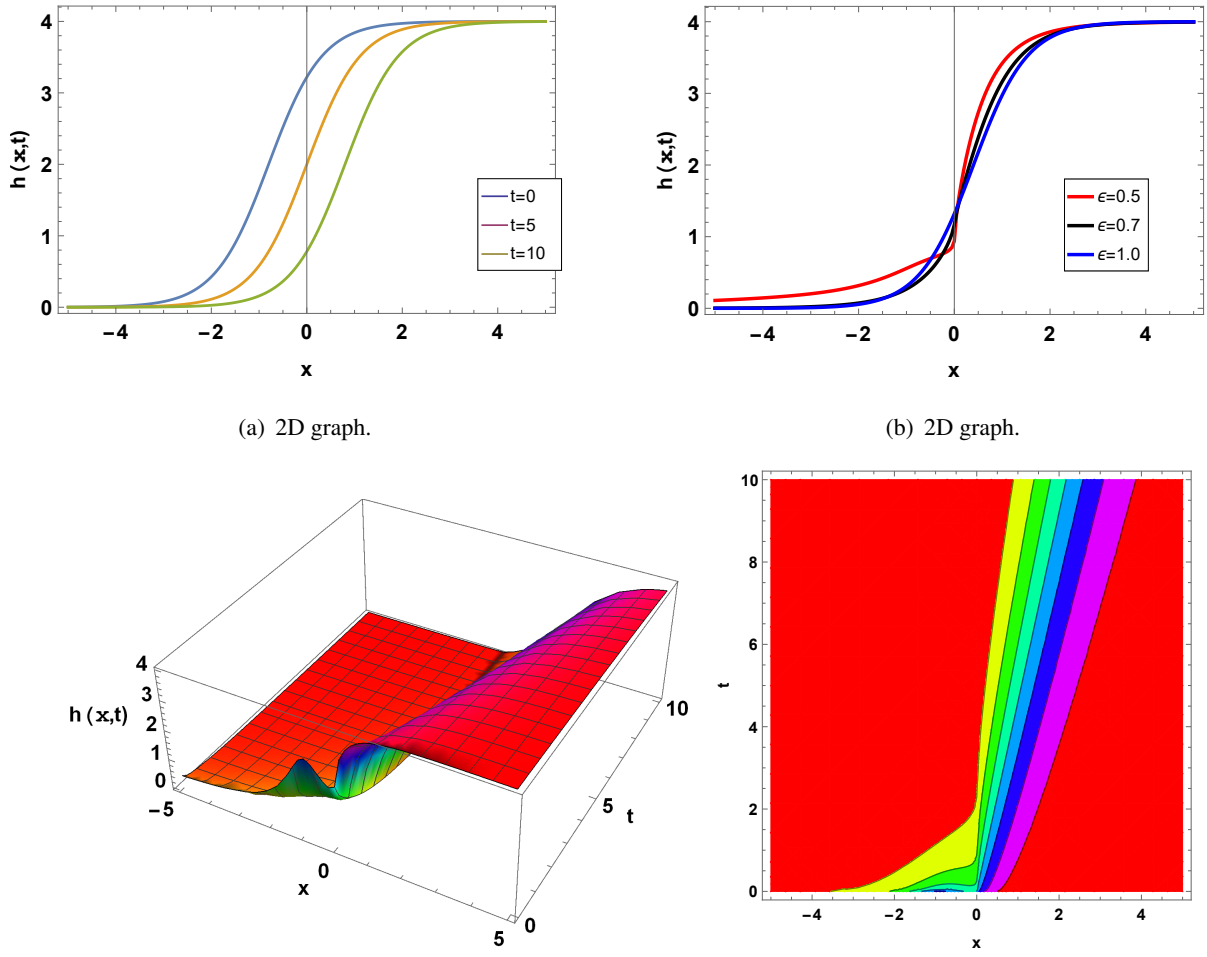

(a) 2D graph.

(b) 2D graph.

(c) 3D plot at $\epsilon = 0.6$

(d) Contour plot when $\epsilon = 0.6$

Figure 3. Physical behavior of $h(x, t)$ denoted through Eq (2.28) for $\theta_3 = 1$, $\theta_4 = -1.8$, $\theta_5 = -0.5$, and $\varrho = 0.5$.

The following graphs denote the kink wave solution. Figure 4a shows the 2D graph for the variation of time when $x \in (-10, 10)$. We can observe that the phase of the wave changes with the change in the values of t. Figure 4b represents the 2D graph for the variation of ϵ when $x \in (-10, 10)$. It is seen that the phase of the wave changes with the change in the value of ϵ. Figure 4c shows the 3D graph for $\epsilon = 0.6$ when $x \in (-10, 10)$ and $t \in (0, 10)$. Figure 4d denotes the contour graph for $\epsilon = 0.6$ when $x \in (-10, 10)$ and $t \in (0, 10)$.

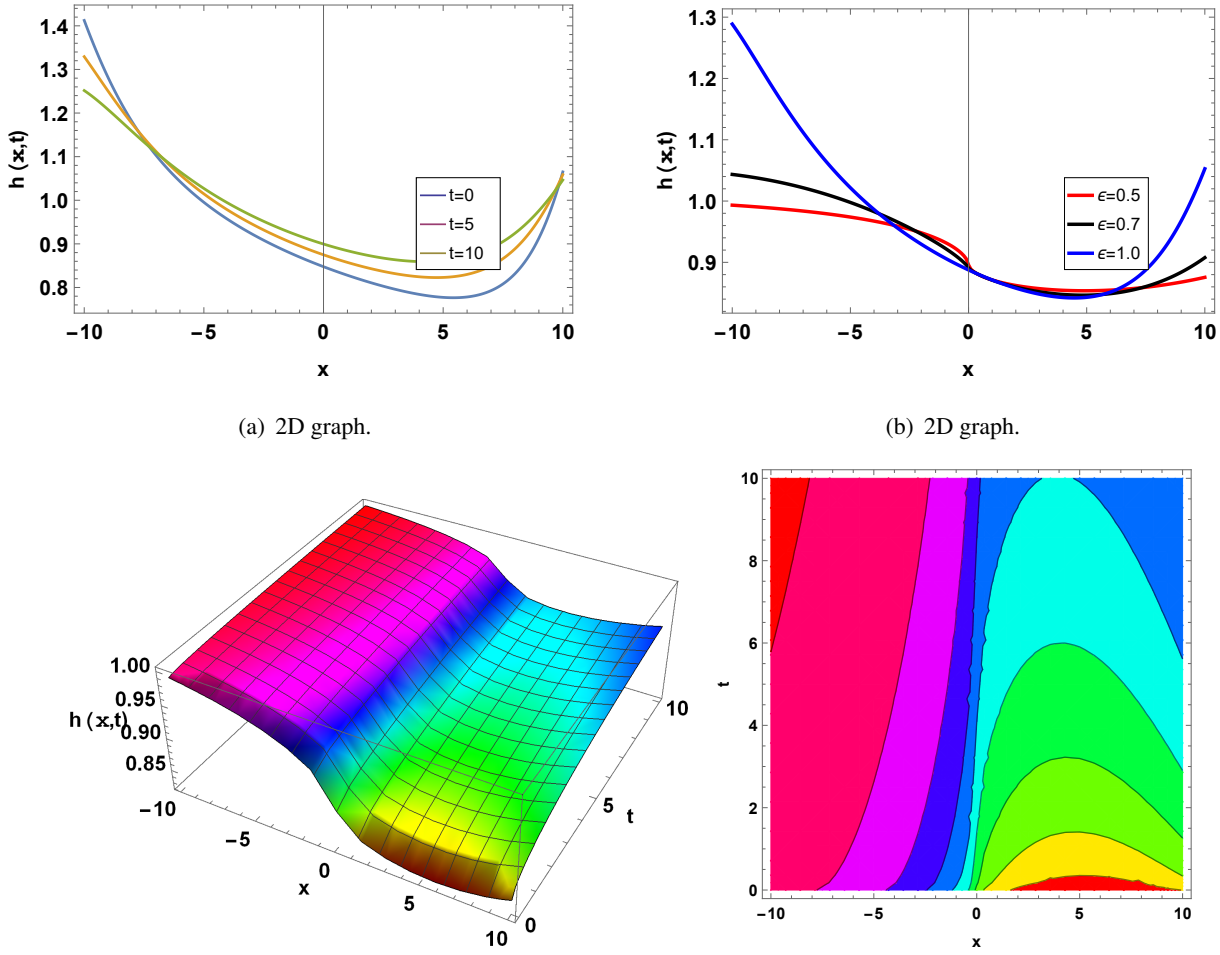

(a) 2D graph.

(b) 2D graph.

(c) 3D plot at $\epsilon = 0.6$

(d) Contour plot when $\epsilon = 0.6$

Figure 4. Physical behavior of $h(x,t)$ denoted through Eq (2.41) for $a = -0.02$, $b = 1$, $\theta_3 = 1$, $\theta_4 = -1.8$, $\theta_5 = 0.5$, $C_1 = 0.5$, $C_2 = -0.2$, and $\varrho = 0.5$.

The following graphs show the periodic wave solution. Figure 5a shows the 2D graph for the variation of time when $x \in (-7, 7)$. It is observed that the phase of the wave changes with the change in the values of t when $x \in (-7, 7)$. Figure 5b represents the 2D graph for the variation of ϵ. It is seen that the phase of the wave changes with the change in the value of ϵ. Figure 5c shows the 3D graph for $\epsilon = 0.6$ when $x \in (-7, 7)$ and $t \in (0, 10)$. Figure 5d denotes the contour graph for $\epsilon = 0.6$ when $x \in (-7, 7)$ and $t \in (0, 10)$.

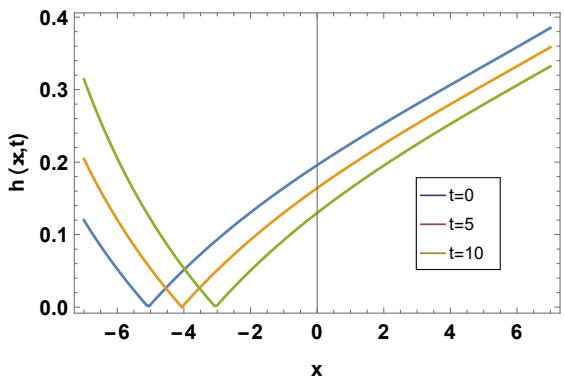

(a) 2D graph.

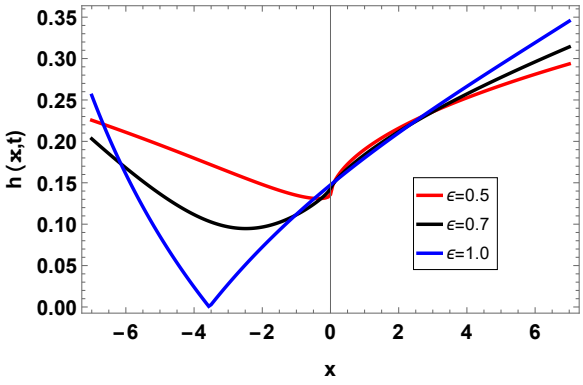

(b) 2D graph.

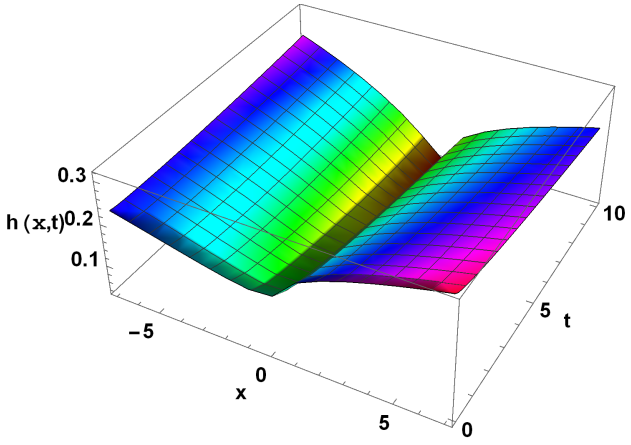

(c) 3D plot at $\epsilon = 0.6$

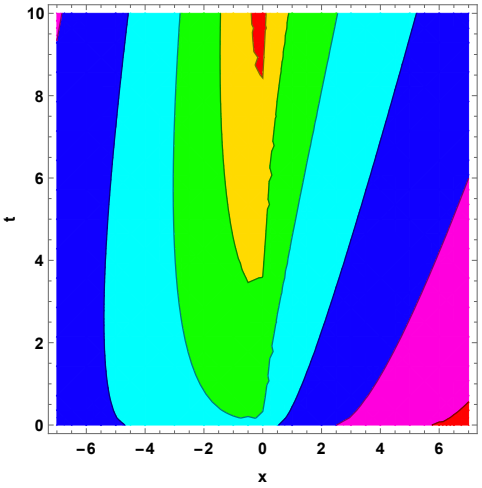

(d) Contour plot when $\epsilon = 0.6$

Figure 5. Physical behavior of $h(x,t)$ denoted through Eq (2.42) when $a = 0.008, b = 1, \theta_3 = 1, \theta_4 = 3, \theta_5 = 0.5, C_1 = 0.1, C_2 = -0.2$, and $\varrho = 0.5$.

4. Qualitative analysis

4.1. Stability analysis

We now describe the stability of the solution. Numerous models, including [48–50], have undergone stability analysis.

We define the Hamiltonian transformation as follows [51]:

$$\mathcal{N} = \frac{1}{2}\int_{-\infty}^{\infty} h^2\, dx, \tag{4.1}$$

where $h(x,t)$ denotes possibility of power while $\mathcal{N}$ denotes the momentum factor. A standard and widely accepted stability condition

$$\frac{\partial \mathcal{N}}{\partial \lambda} > 0 \tag{4.2}$$

is the Vakhitov–Kolokolov stability criterion. Where λ is a fractional wave parameter controlling the propagation scale, putting Eq (2.28) in Eq (4.1) gives

$$\mathcal{N} = \frac{1}{2}\int_{-5}^{5}(-\frac{4}{\theta_3 - 2\theta_5}(1 + \tanh(\Gamma(1+\varrho)(\frac{x^{\epsilon}}{\epsilon} - 2\,(\theta_4 + 2)\,\frac{t^{\epsilon}}{\epsilon}))))^2 dx. \tag{4.3}$$

By using the criterion given in Eq (4.2), we get

$$\begin{aligned}&(8(-t\mathrm{sech}^2(2(\theta_4+2)t+6) + t\mathrm{sech}^2(6-2(\theta_4+2)t) + 2\cosh(2(\theta_4+2)t+6)\mathrm{sech}(6-2(\theta_4+2)t)\\ &(-t\sinh(6-2(\theta_4+2)t)\mathrm{sech}(2(\theta_4+2)t+6) - t\cosh(6-2(\theta_4+2)t)\tanh(2(\theta_4+2)t\\ &+6)\mathrm{sech}(2(\theta_4+2)t+6))))/((\theta_3-2\theta_5)^2) > 0.\end{aligned} \tag{4.4}$$

By putting $\theta_3 = 1$, $\theta_4 = -1.8$, $\theta_5 = -0.5$, and $t = 0$ in the above expression, we get $7.99996 > 0$.

Therefore, the aforementioned condition is met. Hence, the solution is stable.

4.2. Modulation instability analysis

Modulation instability is a phenomenon in which a continuous or plane wave becomes unstable and breaks up into pulses or patterns due to nonlinear effects. This occurs when the interplay between dispersion and nonlinearity leads to the exponential growth of perturbations. Modulation instability has many applications in various fields, such as nonlinear optics, fluid dynamics, and Bose–Einstein condensates.

The steady-state result of the Kudryashov–Sinelshchikov model is examined in [52, 53]:

$$h(x,t) = \left(H(x,t) + \sqrt{\tau}\right)e^{i\tau t}, \tag{4.5}$$

where τ indicates the normalized optical power. Substituting Eq (4.5) into Eq (1.1) and linearizing, one obtains

$$Hi\tau + H_t - \theta_4 H_{xx} + H_{xxx} + i\tau^{3/2} = 0. \tag{4.6}$$

Consider the roots of Eq (4.6) given as follows:

$$H(x,t) = A_1 e^{i(px-qt)} + A_2 e^{-i(px-qt)}, \tag{4.7}$$

where q and p denote constants. Eq (4.7) is put in Eq (4.6). Equating the coefficients of $e^{i(px-qt)}$ and $e^{-i(px-qt)}$, then taking the determinant of the coefficients matrix, we get

$$p^6 + \theta_4^2 p^4 + 2p^3 q + q^2 - \tau^2 = 0. \tag{4.8}$$

The dispersion solution obtained from Eq (4.8) yields

$$q = -p^3 \pm \sqrt{\tau^2 - \theta_4^2 p^4}. \tag{4.9}$$

The solution will be unstable if

$$\tau^2 - \theta_4^2 p^4 < 0. \tag{4.10}$$

The modulation instability gain spectrum $G(p)$ is given as follows:

$$G(p) = 2Im(q) = \pm\sqrt{\tau^2 - \theta_4^2 p^4}. \tag{4.11}$$

5. Results and discussion

Now we present a comparison between our work and previous studies on the governing equation. Various methods have been employed to obtain exact wave solutions of the nonlinear Kudryashov–Sinelshchikov equation. For example, different types of exact solitons were obtained using the (G'/G)-expansion method in [24]. Lump, shock, multi-kink, and singular kink soliton solutions were derived for the fractional Kudryashov–Sinelshchikov equation using the modified extended direct algebraic method in [25]. Various solitary wave solutions were obtained via the modified Khater technique in [26]. Singular bell-shaped, traveling wave, rational, and solitary wave solutions were derived using the generalized exponential rational function method in [27]. Singular, kink, and traveling wave solutions were obtained through the Riccati–Bernoulli sub-ODE method in [28]. Using the Hirota bilinear method, one-, two-, and three-soliton solutions were obtained in [54].

To the best of our knowledge, the governing model has not previously been studied in the framework of the truncated M-fractional derivative. In our work, we employed the modified (G'/G^2)-expansion technique to obtain periodic solitons, kink solitons, and other solutions, while the extended Sinh–Gordon equation expansion method was applied to derive kink–singular, dark, bright, bright–dark, and singular soliton solutions of the equation. The effect of fractional derivatives on the obtained solutions is also discussed as shown in Table 1.

Table 1. Effect of ϵ on wave profile.

ϵ value	Wave amplitude (height)	Wave width	Wave sharpness	Overall effect on profile
1.0	Highest	Narrow	Very sharp	Tall and steep solitary wave
0.7	Medium	Moderate	Moderately sharp	Balanced height and width
0.5	Lowest	Wide	Smooth/Flat	Flattened and spread wave

Similarly, we can draw the above table for the remaining graphs (see Figures 2–5).

Additionally, we performed stability and modulation instability analyses for the model, which are currently active research topics. It is noted that the expansions given in Eqs (2.4), (2.6), and (2.10) can be rewritten as rational functions of an exponential function, which itself may be a solution of an ODE. The expansions in Eqs (2.11) and (2.39) are polynomial expressions in a solution of a Riccati equation, such as Eq (2.12).

6. Conclusions

Finally, we have successfully obtained various types of wave solutions for the nonlinear Kudryashov–Sinelshchikov equation with a truncated M-fractional derivative. By employing the modified (G'/G^2)-expansion method and the extended Sinh–Gordon equation expansion method, we derived solutions expressed in terms of trigonometric, hyperbolic, and rational functions. The exact soliton solutions include periodic, kink, kink–singular, dark, bright, bright–dark, and other forms. These solutions are illustrated using 2D, 3D, and contour plots generated with Mathematica, as shown in Figures 1–5. The obtained results have potential applications in various related fields. The stability of the solutions was confirmed through stability analysis. Using modulation instability analysis, we also obtained the steady-state solutions of the model, and the dynamics of modulation instability are

depicted in Figure 6. The employed techniques are also applicable to other nonlinear fractional PDEs.

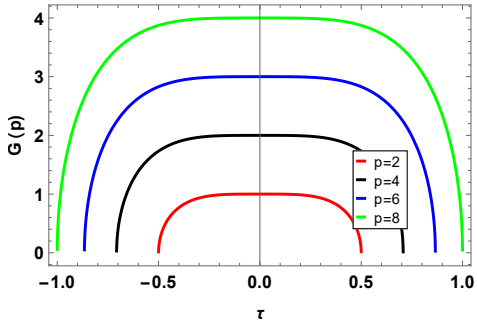

Figure 6. Modulation instability gain spectrum for the value $p = 2, 4, 6, 8$ when $\theta_4 = 4$ and $\tau \in (-2, 2)$. Red graph is for $p = 2$, black graph is for $p = 4$, blue graph is for $p = 6$, and green graph is for $p = 8$.

All the graphs are symmetric about y-axis. So, we can say that the concerned model is stable.

It is well established that solitons arise when dispersive spreading is exactly balanced by nonlinear self-focusing effects. In particular, the bilinear transformation technique provides a systematic framework for deriving multi-soliton solutions and establishing integrability conditions through the so-called Hirota N-soliton criteria.

In the context of the Kudryashov–Sinelshchikov model, the coexistence of higher-order dispersion terms and nonlinear contributions similarly suggests the possibility of stable localized wave structures. Although the present work primarily focuses on constructing exact single-soliton and other analytical solutions via an expansion method, the structure of the reduced equation indicates that, under appropriate parameter constraints, a bilinear representation may be achievable. Consequently, the Hirota N-soliton conditions could potentially be applied to examine the complete integrability and multi-soliton interactions of the model.

These related developments and clarifying that a detailed Hirota bilinear and N-soliton analysis of the Kudryashov–Sinelshchikov equation constitute an interesting direction for future research.

Authors contributions

Haitham Qawaqneh: writing – original draft, conceptualization, methodology; Mostafa Abotaleb: conceptualization, methodology, formal analysis, supervision; Mohammed Ahmed Alomair: writing – review and editing, funding acquisition, project administration; Luai Abdulla Aldoghan: writing – review and editing, methodology. All authors have read and approved the final version of the manuscript for publication.

Use of Generative-AI tools declaration

The authors declare they have not used Artificial Intelligence (AI) tools in the creation of this article.

Fundings

This work was supported by the Deanship of Scientific Research, Vice Presidency for Graduate Studies and Scientific Research, King Faisal University, Saudi Arabia [Grant No.KFU260741].

Conflict of interest

We declare no competing interests in this paper.

References

1. R. Santana-Carrillo, D. Maya-Franco, G. H. Sun, S. H. Dong, Shannon and Fisher entropy for a eew class of single hyperbolic potentials in fractional Schrödinger equation, *Int. J. Quantum Chem.*, **125** (2025), e70024. https://doi.org/10.1002/qua.70024
2. R. Santana-Carrillo, J. M. V. Peto, G. H. Sun, S. H. Dong, Quantum information entropy for a hyperbolic double well potential in the fractional Schrödinger equation, *Entropy*, **25** (2023), 988. https://doi.org/10.3390/e25070988
3. A. Ali, J. Ahmad, S. Javed, Analysis of chaotic structures, bifurcation and soliton solutions to fractional Boussinesq model, *Phys. Scr.*, **98** (2023), 075217. https://doi.org/10.1088/1402-4896/acdcee
4. W. W. Mohammed, C. Cesarano, N. Iqbal, R. Sidaoui, E. E. Ali, The exact solutions for the fractional Riemann wave equation in quantum mechanics and optics, *Phys. Scr.*, **99** (2024), 085245. https://doi.org/10.1088/1402-4896/ad62a3
5. H. Qawaqneh, K. H. Hakami, A. Altalbe, M. Bayram, The discovery of truncated m-fractional exact solitons and a qualitative analysis of the generalized bretherton model, *Mathematics*, **12** (2024), 2772. https://doi.org/10.3390/math12172772
6. I. M. Batiha, S. A. Njadat, R. M. Batyha, A. Zraiqat, A. Dababneh, S. Momani, Design fractional-order PID controllers for single-joint robot arm model, *Int. J. Adv. Soft Comput. Appl.*, **14** (2022), 96–114. https://doi.org/10.15849/IJASCA.220720.07
7. M. D. Junjua, S. Altaf, A. A. Alderremy, E. E. Mahmoud, Exact wave solutions of truncated M-fractional Boussinesq–Burgers system via an effective method, *Phys. Scr.*, **99** (2024), 095263. https://doi.org/10.1088/1402-4896/ad6ec9
8. S. Akram, J. Ahmad, S. U. Rehman, T. Younas, Stability analysis and dispersive optical solitons of fractional Schrödinger–Hirota equation, *Opt. Quantum Electron.*, **55** (2023), 664. https://doi.org/10.1007/s11082-023-04942-2
9. H. Qawaqneh, Y. Alrashedi, Mathematical and physical analysis of fractional Estevez-Mansfield-Clarkson equation, *Fractal Fract.*, **8** (2024), 467. https://doi.org/10.3390/fractalfract8080467
10. Y. H. Liang, K. J. Wang, The modified variational principles of the fractal Rosenau–Burgers equation, *Fractals*, 2026. https://doi.org/10.1142/S0218348X26500532
11. K. J. Wang, An effective computational approach to the local fractional low-pass electrical transmission lines model, *Alex. Eng. J.*, **110** (2025), 629–635. https://doi.org/10.1016/j.aej.2024.07.021

12. S. Akram, J. Ahmad, S. U. Rehman, S. Alkarni, N. A. Shah, Exploration of solitary wave solutions of highly nonlinear KDV–KP equation arise in water wave and stability analysis, *Results Phys.*, **54** (2023), 107054. https://doi.org/10.1016/j.rinp.2023.107054

13. L. Cheng, W. X. Ma, Soliton and lump solutions to a fourth-order nonlinear wave equation in (2+1)-dimensions, *Qual. Theory Dyn. Syst.*, **24** (2025), 237. https://doi.org/10.1007/s12346-025-01384-x

14. K. J. Wang, S. Li, K. H. Yan, Resonant multiple wave, multi-lump wave and complex N-soliton solutions to the (3+1)-dimensional Jimbo–Miwa equation, *Mod. Phys. Lett. B*, **40** (2026), 2650001. https://doi.org/10.1142/S0217984926500016

15. A. R. Seadawy, A. Ali, A. Bekir, Exact wave solutions of new generalized Bogoyavlensky–Konopelchenko model in fluid mechanics, *Mod. Phys. Lett. B*, **38** (2024), 2450262. https://doi.org/10.1142/S0217984924502622

16. M. N. Qureshi, A. H. Soori, Z. Haider, W. A. Khan, Z. Arshad, Exact solutions of the damped telegrapher's equation with harmonic potential via the generalized first integral method, *Eur. J. Pure Appl. Math.*, **18** (2025), 6325–6325. https://doi.org/10.29020/nybg.ejpam.v18i3.6325

17. K. F. Al Oweidi, H. A. Aal-Rkhais, Existence results for a nonlinear degenerate parabolic equation involving-Laplacian type diffusion process, *Iraqi J. Sci.*, **65** (2024), 5081–5094. https://doi.org/10.24996/ijs.2024.65.9.24

18. H. Qawaqneh, A. Zafar, M. Raheel, A. A. Zaagan, E. H. M. Zahran, A. Cevikel, et al., New soliton solutions of M-fractional Westervelt model in ultrasound imaging via two analytical techniques, *Opt. Quantum Electron.*, **56** (2024), 737. https://doi.org/10.1007/s11082-024-06371-1

19. K. J. Wang, K. H. Yan, S. Li, Variational principle of the zig-zag optical lattice model in quantum physics, *Mod. Phys. Lett. A*, **41** (2026), 2550221. https://doi.org/10.1142/S0217732325502219

20. K. J. Wang, K. H. Yan, F. Shi, G. Li, X. L. Liu, Qualitative study of the (2+1)-dimensional BLMPE equation: variational principle, Hamiltonian and diverse wave solutions, *AIMS Math.*, **10** (2025), 26168–26186. https://doi.org/10.3934/math.20251152

21. Y. H. Liang, K. J. Wang, Resonant multiple soliton, non-singular complexiton and singular complexiton solutions to the (3+1)-dimensional shallow water wave equation, *Int. J. Comput. Math.*, 2026. https://doi.org/10.1080/00207160.2025.2608755

22. H. A. Aal-Rkhais, A. H. Kamil, K. F. A. Oweidi, The approximation of weighted Hölder functions by Fourier-Jacobi polynomials to the singular Sturm-Liouville operator, *Baghdad Sci. J.*, **19** (2022), 6. https://doi.org/10.21123/bsj.2022.6128

23. N. A. Kudryashov, D. I. Sinelshchikov, Nonlinear waves in bubbly liquids with consideration for viscosity and heat transfer, *Phys. Lett. A*, **374** (2010), 2011–2016. https://doi.org/10.1016/j.physleta.2010.02.067

24. J. Lu, New exact solutions for Kudryashov–Sinelshchikov equation, *Adv. Differ. Equations*, **2018** (2018), 374. https://doi.org/10.1186/s13662-018-1769-6

25. R. Ali, A. S. Hendy, M. R. Ali, A. M. Hassan, F. A. Awwad, E. A. A. Ismail, Exploring propagating soliton solutions for the fractional Kudryashov–Sinelshchikov equation in a mixture of liquid-gas bubbles under the consideration of heat transfer and viscosity, *Fractal Fract.*, **7** (2023), 773. https://doi.org/10.3390/fractalfract7110773

26. C. Yue, M. M. A. Khater, R. A. M. Attia, D. Lu, The plethora of explicit solutions of the fractional KS equation through liquid-gas bubbles mix under the thermodynamic conditions via Atangana-Baleanu derivative operator, *Adv. Differ. Equations*, **2020** (2020), 62. https://doi.org/10.1186/s13662-020-2540-3

27. S. Kumar, M. Niwas, S. K. Dhiman, Abundant analytical soliton solutions and different wave profiles to the Kudryashov–Sinelshchikov equation in mathematical physics, *J. Ocean Eng. Sci.*, **7** (2022), 565–577. https://doi.org/10.1016/j.joes.2021.10.009

28. M. Inc, A. I. Aliyu, A. Yusuf, D. Baleanu, New solitary wave solutions and conservation laws to the Kudryashov–Sinelshchikov equation, *Optik*, **142** (2017), 665–673. https://doi.org/10.1016/j.ijleo.2017.05.055

29. M. S. Bruzón, E. Recio, R. de la Rosa, M. L. Gandarias, Local conservation laws, symmetries, and exact solutions for a Kudryashov–Sinelshchikov equation, *Math. Methods Appl. Sci.*, **41** (2018), 1631–1641. https://doi.org/10.1002/mma.4690

30. A. H. Hazza, W. M. Taha, R. A. Hameed, I. A. Ibrahim, New solitary solution for the Kudryashov–Sinelshchikov (KS) equation by modern extension of the hyperbolic method, *Tikrit J. Pure Sci.*, **25** (2020), 124–128. https://doi.org/10.25130/J.V25I2.967

31. S. B. G. Karakoc, A. Saha, S. K. Bhowmik, D. Y. Sucu, Numerical and dynamical behaviors of nonlinear traveling wave solutions of the Kudryashov–Sinelshchikov equation, *Wave Motion*, **118** (2023), 103121. https://doi.org/10.1016/j.wavemoti.2023.103121

32. C. R. Jisha, R. K. Dubey, D. Benton, A. Rashid, The exact solutions for Kudryashov and Sinelshchikov equation with variable coefficients, *Phys. Scr.*, **97** (2022), 095212. https://doi.org/10.1088/1402-4896/ac89ba

33. T. Ak, M. S. Osman, A. H. Kara, Polynomial and rational wave solutions of Kudryashov–Sinelshchikov equation and numerical simulations for its dynamic motions, *J. Appl. Anal. Comput.*, **10** (2020), 2145–2162. https://doi.org/10.11948/20190341

34. A. F. Alharbi, U. Akram, Ansatz-based exploration of M-shaped and multi-wave solitons in the Kudryashov–Sinelshchikov model, *Mod. Phys. Lett. B*, **39** (2025), 2550169. https://doi.org/10.1142/S0217984925501696

35. D. Kumar, J. Manafian, F. Hawlader, A. Ranjbaran, New closed form soliton and other solutions of the Kundu-Eckhaus equation via the extended sinh-Gordon equation expansion method, *Optik*, **160** (2018), 159–167. https://doi.org/10.1016/j.ijleo.2018.01.137

36. A. Irshad, N. Ahmed, U. Khan, S. T. Mohyud-Din, I. Khan, E. S. M. Sherif, Optical solutions of Schrödinger equation using extended Sinh–Gordon equation expansion method, *Front. Phys.*, **8** (2020), 73. https://doi.org/10.3389/fphy.2020.00073

37. F. Batool, H. Rezazadeh, Z. Ali, U. Demirbilek, Exploring soliton solutions of stochastic Phi-4 equation through extended Sinh–Gordon expansion method, *Opt. Quantum Electron.*, **56** (2024), 785. https://doi.org/10.1007/s11082-024-06385-9

38. K. K. Ali, M. Raheel, M. Inc, Some new types of optical solitons to the time-fractional new hamiltonian amplitude equation via extended Sinh–Gordon equation expansion method, *Mod. Phys. Lett. B*, **36** (2022), 2250089. https://doi.org/10.1142/S0217984922500890

39. N. H. Aljahdaly, Some applications of the modified (G'/G^2)-expansion method in mathematical physics, *Results Phys.*, **13** (2019), 102272. https://doi.org/10.1016/j.rinp.2019.102272

40. S. Behera, N. H. Aljahdaly, J. P. S. Virdi, On the modified (G'/G^2)-expansion method for finding some analytical solutions of the traveling waves, *J. Ocean Eng. Sci.*, **7** (2022), 313–320. https://doi.org/10.1016/j.joes.2021.08.013

41. A. Mumtaz, M. Shakeel, A. Manan, N. A. Shah, S. F. Ahmed, A comparative study of new traveling wave solutions for the (2+1)-dimensional fractional Wazwaz Kaur Boussinesq equation using novel modified (G'/G^2)-expansion method, *AIP Adv.*, **15** (2025), 035204. https://doi.org/10.1063/5.0253219

42. S. Behera, D. Behera, Nonlinear wave dynamics of (1+1)-dimensional conformable coupled nonlinear Higgs equation using modified (G'/G^2)-expansion method, *Phys. Scr.*, 2025. https://doi.org/10.1088/1402-4896/adaa31

43. T. A. Sulaiman, G. Yel, H. Bulut, M-fractional solitons and periodic wave solutions to the Hirota-Maccari system, *Mod. Phys. Lett. B*, **33** (2019), 1950052. https://doi.org/10.1142/S0217984919500520

44. J. V. C. Sousa, E. C. Oliveira, A new truncated M-fractional derivative type unifying some fractional derivative types with classical properties, *Int. J. Anal. Appl.*, **16** (2018), 83–96.

45. Z. Yan, A Sinh-Gordon equation expansion method to construct doubly periodic solutions for nonlinear differential equations, *Chaos Solitons Fract.*, **16** (2003), 291–297. https://doi.org/10.1016/S0960-0779(02)00321-1

46. X. L. Yang, J. S. Tang, Travelling wave solutions for Konopelchenko–Dubrovsky equation using an extended Sinh–Gordon equation expansion method, *Commun. Theor. Phys.*, **50** (2008), 1047–1051. https://doi.org/10.1088/0253-6102/50/5/06

47. Y. Zhang, J. Pang, L. Zhang, Application of (G'/G^2)-expansion method for solving Schrödinger's equation with three-order dispersion, *Adv. Appl. Math.*, **6** (2017), 212–217. https://doi.org/10.12677/aam.2017.62024

48. H. Qawaqneh, H. A. Jari, A. Altalbe, A. Bekir, Stability analysis, modulation instability, and the analytical wave solitons to the fractional Boussinesq–Burgers system, *Phys. Scr.*, **99** (2024), 125235. https://doi.org/10.1088/1402-4896/ad8e07

49. K. U. Tariq, A. M. Wazwaz, R. Javed, Construction of different wave structures, stability analysis and modulation instability of the coupled nonlinear Drinfel'd–Sokolov–Wilson model, *Chaos Solitons Fract.*, **166** (2023), 112903. https://doi.org/10.1016/j.chaos.2022.112903

50. H. Zulfiqar, A. Aashiq, K. U. Tariq, H. Ahmad, B. Almohsen, M. Aslam, et al., On the solitonic wave structures and stability analysis of the stochastic nonlinear Schrödinger equation with the impact of multiplicative noise, *Optik*, **289** (2023), 171250. https://doi.org/10.1016/j.ijleo.2023.171250

51. N. G. Vakhitov, A. A. Kolokolov, Stationary solutions of the wave equation in the medium with nonlinearity saturation, *Radiophys. Quantum Electron.*, **16** (1973), 783–789. https://doi.org/10.1007/BF01031343

52. H. Qawaqneh, J. Manafian, M. Alharthi, Y. Alrashedi, Stability analysis, modulation instability, and beta-time fractional exact soliton solutions to the Van der Waals equation, *Mathematics*, **12** (2024), 2257. https://doi.org/10.3390/math12142257

53. S. ur Rehman, J. Ahmad, Modulation instability analysis and optical solitons in birefringent fibers to RKL equation without four wave mixing, *Alex. Eng. J.*, **60** (2021), 1339–1354. https://doi.org/10.1016/j.aej.2020.10.055

54. S. Barik, S. Behera, Soliton solutions with stability, bifurcation analysis and phase portraits of Kudryashov–Sinelshchikov equation, *Chaos Solitons Fract.*, **201** (2025), 117367. https://doi.org/10.1016/j.chaos.2025.117367

AIMS Press